Published in final edited form as:
NMR Biomed. 2012 September ; 25(9): 1073–1087. doi:10.1002/nbm.2772.

Increased ventricular lactate in chronic fatigue syndrome. III. Relationships to cortical glutathione and clinical symptoms implicate oxidative stress in disorder pathophysiology

Dikoma C. Shungu[a,*], **Nora Weiduschat**[a], **James W. Murrough**[b], **Xiangling Mao**[a], **Sarah Pillemer**[b], **Jonathan P. Dyke**[a], **Marvin S. Medow**[c], **Benjamin H. Natelson**[d], **Julian M. Stewart**[c], and **Sanjay J. Mathew**[b,e]

[a] Department of Radiology, Weill Medical College of Cornell University, New York, NY, USA

[b] Department of Psychiatry, Mount Sinai School of Medicine, New York, NY, USA

[c] Center for Hypotension, New York Medical College, Valhalla, NY, USA

[d] Department of Pain Medicine and Palliative Care, Beth Israel Medical Center, New York, NY, USA

[e] Department of Psychiatry and Behavior Sciences, Baylor College of Medicine, Houston, TX, USA

Abstract

Chronic fatigue syndrome (CFS) is a complex illness, which is often misdiagnosed as a psychiatric illness. In two previous reports, using ^{1}H MRSI, we found significantly higher levels of ventricular cerebrospinal fluid (CSF) lactate in patients with CFS relative to those with generalized anxiety disorder and healthy volunteers (HV), but not relative to those with major depressive disorder (MDD). In this third independent cross-sectional neuroimaging study, we investigated a pathophysiological model which postulated that elevations of CSF lactate in patients with CFS might be caused by increased oxidative stress, cerebral hypoperfusion and/or secondary mitochondrial dysfunction. Fifteen patients with CFS, 15 with MDD and 13 HVs were studied using the following modalities: (i) ^{1}H MRSI to measure CSF lactate; (ii) single-voxel ^{1}H MRS to measure levels of cortical glutathione (GSH) as a marker of antioxidant capacity; (iii) arterial spin labeling (ASL) MRI to measure regional cerebral blood flow (rCBF); and (iv) ^{31}P MRSI to measure brain high-energy phosphates as objective indices of mitochondrial dysfunction. We found elevated ventricular lactate and decreased GSH in patients with CFS and MDD relative to HVs. GSH did not differ significantly between the two patient groups. In addition, we found lower rCBF in the left anterior cingulate cortex and the right lingual gyrus in patients with CFS relative to HVs, but rCBF did not differ between those with CFS and MDD. We found no differences between the three groups in terms of any high-energy phosphate metabolites. In exploratory correlation analyses, we found that levels of ventricular lactate and cortical GSH were inversely correlated, and significantly associated with several key indices of physical health and disability. Collectively, the results of this third independent study support a pathophysiological model of CFS in which increased oxidative stress may play a key role in CFS etiopathophysiology.

[*] Correspondence to: D. C. Shungu, Professor of Physics in Radiology, Citigroup Biomedical Imaging Center, Weill Medical College of Cornell University, 516 E 72nd Street, New York, NY 10021, USA. dcs7001@med.cornell.edu.

Keywords

MRS; lactate; cerebrospinal fluid; glutathione; arterial spin labeling; cerebral blood flow; chronic fatigue syndrome; major depressive disorder

INTRODUCTION

Chronic fatigue syndrome (CFS) is a medically unexplained illness, diagnosed only after alternative medical and neuropsychiatric pathologies have been excluded. The pathognomonic symptom of CFS is debilitating fatigue lasting for at least 6 months, which is accompanied by at least four of eight infectious, rheumatologic or neuropsychiatric symptoms (1,2). The diagnosis remains controversial because of the disorder's heterogeneous phenomenology, extensive overlap with neuropsychiatric symptoms and lack of validated diagnostic tests. As a result, the discovery of CFS-specific biomarkers is currently an area of intense research.

In two previous studies, we used ^{1}H MRSI to compare neurometabolites in CFS with those in generalized anxiety disorder (3) and major depressive disorder (MDD) (4), common neuro-psychiatric disorders with extensive symptom overlap with CFS. In these reports, patients with CFS showed significantly elevated ventricular cerebrospinal fluid (CSF) lactate relative to healthy controls (3,4) and to patients with generalized anxiety disorder (3), whereas no differences were found between patients with CFS and MDD (4). Importantly, our replicated finding of significant elevations of ventricular lactate in CFS (3,4) suggested a potential illness-associated biomarker, whose understanding could shed new light onto the pathophysiology of the illness.

In this study, we investigated a pathophysiological model of CFS, which postulates that sustained oxidative stress (5) and associated oxidant damage (6,7) lead to cerebral hypoperfusion (8–11) and/or to secondary mitochondrial dysfunction (5) which could potentially explain our observed cross-sectional elevations of ventricular lactate (3,4). Specifically, this study had two primary objectives: (i) to use ^{1}H MRSI to replicate, in a new cohort, our finding of cross-sectional elevations of ventricular lactate in CFS (3,4); and (ii) to determine whether the postulated (5) and experimentally documented (6,7) oxidative stress increases in the disorder are associated with antioxidant capacity deficit using ^{1}H MRS to measure *in vivo* brain levels of glutathione (GSH), the most abundant antioxidant in the central nervous system (12). Our secondary aims were as follows: (i) to use arterial spin labeling (ASL) MRI (13) to replicate previous observations of decreased regional cerebral blood flow (rCBF) in CFS (8–11), which may explain the observed lactate elevations; (ii) to use ^{31}P MRSI to measure regional brain levels of high-energy phosphates (e.g. ATP) as indices of a possible secondary mitochondrial dysfunction in CFS (5), whose presence might also be associated with elevations in lactate; and (iii) to assess whether these neuroimaging markers correlate with clinical characteristics in CFS.

All neuroimaging studies were conducted in a single 90–120-min examination, enabling the acquisition of temporally concordant data for potentially more meaningful comparisons between the outcome measures. As in our previous studies (3,4), age- and sex-matched healthy volunteers (HVs) and patients with MDD served as normal controls and ‘disease controls’, respectively.

MATERIALS AND METHODS

Subjects enrolled into the study provided written informed consent before all procedures, and were compensated for their participation. Diagnostic and laboratory assessments for patients with MDD and HVs were conducted at Mount Sinai School of Medicine, and those for patients with CFS were conducted at Beth Israel Medical Center. All neuroimaging scans and additional day-of-scan clinical evaluations were performed at Weill Cornell Medical College. Approval to conduct the studies was granted by the institutional review boards of the participating institutions.

Subjects

For all participants, general eligibility requirements included age between 18 and 45 years, negative urine toxicology at screening and on the day of scan and, for females of reproductive age, the use of an effective birth control method and negative day-of-scan pregnancy test. In addition, all participants were instructed to refrain from the consumption of alcohol for at least 48 h prior to the neuroimaging scans, as the measured lactate CH_3 group has nearly the same MR frequency as the ethanol CH_3 group at 1.3 ppm. Exclusion criteria consisted of any unstable medical or neurological illness or any condition precluding MRI exposure (e.g. pacemaker, metallic prosthesis). All participants were assessed for psychiatric disorders using the Structured Clinical Interview for the Diagnostic and Statistical Manual of Mental Disorders, 4th edn. (14).

Patients with CFS were recruited via clinician referrals and media advertisements and were diagnosed by a board-certified neurologist with extensive CFS research experience (BHN), using modified US Centers for Disease Control and Prevention (CDC) guidelines (1). Patients with MDD were recruited through similar methods and were evaluated by a board-certified psychiatrist (SJM or JWM). All participants had been psychotropic medication free for 2 weeks or more (≥ 4 weeks for fluoxetine) prior to the scans, had been free of substance abuse/dependence for 6 months or more, had no lifetime history of psychotic disorder, mania or hypomania, had no pervasive developmental disorder or mental retardation, and had no current eating disorder. HVs, recruited through local media advertisement, did not meet the criteria for CFS or any psychiatric disorder, and were group matched for sex and age to the two patient groups.

Clinical assessments

Within 1 week of the scan, participants underwent a standardized clinical assessment battery, which included the following: (i) CDC Symptom Inventory for CFS symptoms (1); (ii) fatigue severity using the 20-item Multidimensional Fatigue Inventory (MFI) (15); (iii) physical and mental health using the 36-Item Short Form Health Survey by the RAND Corporation, Santa Monica, CA, USA (RAND SF-36) (16); (iv) functional impairment and disability using the Sheehan Disability Scale (SDS) (17); (v) pain and interference of pain with activities of daily life using the Wisconsin Brief Pain Inventory (18); (vi) sleep quality using the Pittsburgh Sleep Quality Index (19); (vii) depression using the Quick Inventory of Depressive Symptomatology – Self Report (QIDS-SR) (20); and (viii) early life traumatic events using the Childhood Trauma Questionnaire (21).

Ventricular lactate and volume measurements by ^{1}H MRSI and structural MRI

All neuroimaging studies were conducted on a research-dedicated, multinuclear, General Electric 3.0-T EXCITE MR system at Weill Cornell Medical College.

The *in vivo* levels of ventricular lactate and the lateral ventricular volume (Fig. 1) which contributed signal to the measured lactate were obtained in all subjects using a commercial,

double-quadrature, dual-tuned, $^{1}H/^{31}P$ head coil (Clinical MR Solutions, LLC, Brookfield, WI, USA), employing a multislice ^{1}H MRSI technique (22) and volumetric analysis of structural MRI data acquired with a standard three-dimensional, T_1-weighted, spoiled gradient-recalled echo technique, respectively, as described previously (3,4). The lactate levels presented are the mean values obtained for all voxels in the ventricular space (Fig. 1A, C), expressed in institutional units (i.u.) as ratios relative to the root-mean-square (rms) of the background noise in the spectra, and corrected for the contribution of finite noise at the lactate frequency to ensure a mean lactate value of 0.0 ± SD for the HV group (4). Negative lactate values thus simply re flect random noise fluctuations at the lactate frequency (4).

Single-slice ^{31}P MRSI data acquisition protocol

^{31}P MRSI data were recorded with the same dual-tuned, double-quadrature, $^{1}H/^{31}P$ volume head coil as used for the ^{1}H MRSI scans from a single 30-mm slice, prescribed to be co-axial with the central slice in the ^{1}H MRSI lactate scan (Fig. 1A), thereby ensuring overlap of the regions of interest in the two scans for enhanced correlation. A pulse sequence ('FIDCSI') supplied by the instrument manufacturer and consisting of a single slice-selective radiofrequency (RF) pulse, followed by a slice refocusing gradient and phase-encoding gradients, was implemented with 14 × 14 phase-encoding steps, a field of view of 420 mm, 2048 sample points, a spectral width of 5 kHz, TR = 1000 ms and eight excitations per phase-encoding step, to yield voxels with a nominal size of 3.0 × 3.0 × 3.0 cm^3 in a total scan time of 26 min. The field homogeneity in the ^{31}P MRSI slice was automatically optimized by the host computer on the water ^{1}H signal from the same slice detected with the ^{1}H coil prior to initiating the ^{31}P acquisition. The raw data matrix size was zero filled to 32 × 32 spatial points prior to standard three-dimensional Fourier transformation to yield a grid of spectral voxels (Fig. 2) which was selected for further post-processing and statistical analysis. Although our use of a relatively short TR (1000 ms) probably resulted in substantial saturation of all ^{31}P resonances, this did not adversely affect the signal-to-noise ratio (Fig. 2).

Brain GSH measurement by ^{1}H MRS and assessment of voxel brain matter content

Following the ^{1}H and ^{31}P MRSI scans, the dual-tuned $^{1}H/^{31}P$ head coil was replaced with an eight-channel phased-array head coil to measure levels of GSH in 15 min from a single 3 × 3 × 2-cm^3 occipital cortex (OCC) voxel (Fig. 3A), a region in which we had previously found abnormal levels of γ-aminobutyric acid (GABA) in patients with MDD (32), and is thus of interest as depressive symptoms are common among CFS sufferers. It should be noted that, because of its low brain concentration (0.5–1.5 mmol/L) and overlap by a total creatine (tCr) resonance at 3.0 ppm, which is up to 10-fold stronger (Fig. 3B, spectrum a), *in vivo* brain GSH is technically challenging to detect by ^{1}H MRS. However, using the *J*-edited spin echo difference technique (23,24), we reliably achieved unobstructed detection of the GSH β-cysteinyl resonance at 2.98 ppm in this study (Fig. 3B, C). Briefly, a standard point-resolved spectroscopy sequence was turned into a volume-selective *J*-editing sequence by inserting a pair of frequency-selective inversion RF pulses, flanked by spoiler gradient pulses of opposite signs, before and after the second 180° RF pulse of the double spin echo. The application of these 'editing' RF pulses at the frequency (4.56 ppm) of the GSH α-cysteinyl resonance on alternate scans, with TE/TR = 68/1500 ms, alternately inverts the GSH β-cysteinyl resonance at 2.98 ppm by inhibiting and allowing its J modulation. The subtraction of the two sub-spectra acquired yields the desired GSH resonance at 2.98 ppm (Fig. 3B), with complete elimination of the overlapping tCr singlet, which is not J modulated. Figure 3C shows a stacked plot of edited spectra from five subjects, with the GSH peak clearly and consistently detected at 2.98 ppm. To obtain the area under this peak, a robust and highly optimized public-domain Levenberg–Marquardt nonlinear least-squares minimization

routine (25), written in Interactive Data Language (IDL; Visual Information Solutions, Boulder, CO, USA), was implemented to selectively fit the GSH resonance in the frequency domain (Fig. 3B, spectrum d) to a pseudo-Voigt function, which enables more precise analysis of resonances that consist of mixtures of Lorentzian and Gaussian lineshapes (26), as is often the case for *in vivo* spectra. For group comparisons and reporting, the resulting GSH peak areas were expressed semi-quantitatively as ratios relative to the area of the simultaneously acquired unsuppressed water resonance (W) in the OCC voxel.

As metabolite level differences have been reported between gray matter (GM) and white matter (WM) (27,28), we implemented volumetric MRI-based tissue segmentation to assess brain matter content and heterogeneity of our relatively large OCC voxel. MEDx software (Medical Numerics, Sterling, VA, USA) was used to segment the brain tissue based on the signal intensity histogram of each subject's volumetric (spoiled gradient-recalled echo) MRI. From the histogram, a segmentation mask of the OCC voxel was generated and the proportions of GM, WM and CSF for the voxel were computed. These were then compared between groups for use as covariates in the case of significant differences.

rCBF measurements using ASL MRI

rCBF was measured in each participant with the same eight-channel head coil as used for the GSH scans, employing a pseudo-continuous spiral gradient echo ASL pulse sequence (13). A field of view of 24 cm and an acquisition matrix of 512 × 8 resulted in a reconstructed matrix of 128 × 128 and a resolution of 0.53 mm × 0.53 mm × 3.8 mm over 48 slices. Acquisition parameters included TR/TE = 10.4/2.4 ms, a labeling delay of 1500 ms and a bandwidth of 62.5 kHz, resulting in a total scan time of 5.25 min. Water spins were labeled at the cervico-medullary junction, approximately 1 cm superior to the cerebellum, using velocity-driven adiabatic inversion with an amplitude-modulated control labeling pulse, which reproduces the frequency-dependent off-resonance effects of the labeling pulse, and therefore permits multislice imaging. A fast T_1 map was generated using the same sequence to allow the quantification of rCBF. A reference T_1-weighted anatomic imaging series, matching the ASL acquisition in slice placement and thickness, was acquired for anatomical reference. Finally, an axial, high-resolution, isotropic, three-dimensional BRAVO (BRAin VOlume imaging) sequence was acquired with a spatial resolution of 1.1 mm × 1.1 mm × 1.5 mm. Acquisition parameters included TR/TE/TI = 8.3/1.6/725 ms, a flip angle of 7°, field of view of 24 cm, matrix of 256 × 192 and 124 slices for overlay of the rCBF data.

rCBF maps were calculated in real time on the MRI scanner to solve the following equation pixel by pixel:

$$\mathrm{rCBF}=\frac{\lambda}{T_{1\mathrm{app}}}\frac{M_{\mathrm{control}}-M_{\mathrm{tagged}}}{2M_{\mathrm{control}}}$$

where λ represents the brain–blood partition coefficient reflecting the water distribution between intravascular and extravascular compartments, and has been determined to assume the value of 0.9 mL/g, $T_{1\mathrm{app}}$ is the apparent T_1 of tissue as altered by the labeled blood, and M_{control} and M_{tagged} are the longitudinal magnetizations per gram of brain tissue for the control and tagged acquisitions derived from recorded ASL data.

The resulting rCBF images were normalized to the Montreal Neurological Institute positron emission tomography template using Statistical Parametric Mapping software version 5 (Wellcome Department of Imaging Neuroscience, London, UK). An 8-mm smoothing kernel was applied to the source images during normalization. A Bayesian framework was used to determine the optimal 12-parameter affine transformation needed to normalize the

rCBF image set to the Montreal Neurological Institute template. Groupwise voxel-based analysis of the ASL data was performed, followed by between-group *t*-test comparisons in which age and gender were regressed out of the model as independent covariates. The threshold on voxel-level rCBF values was set at an uncorrected $p \leq 0.001$.

Statistical analysis

Prior to the analyses, the normality of all data was assessed using the Shapiro–Wilks test. The Type I error rate (i.e. chance findings) was protected against by limiting the statistical tests only to our specified hypotheses. Differences in the means of the primary outcome measures (GSH and CSF lactate) between the three groups were assessed using one-way analysis of variance (ANOVA), with Bonferroni correction for multiple comparisons. For all normally distributed secondary outcome measures, three-group comparisons were performed using general linear models (ANOVA), followed by post-hoc comparisons with Tukey's honestly significant difference test. Additional factors and covariates were chosen based on their previously reported influence on MRS markers. In the case of inhomogeneity of variance, Welch tests were performed for global group comparisons and Games–Howell tests for *post-hoc* pairwise comparisons.

Group comparisons for non-normally distributed data used the Kruskal–Wallis nonparametric test, with Mann–Whitney *U*-tests for *post-hoc* analyses. Exploratory associations between continuous variables were conducted using Pearson's product–moment correlation (*r*) or, for non-normally distributed data, Spearman ρ. All analyses were two-tailed, with the level of significance set at $\alpha < 0.05$, unless otherwise noted. All statistical analyses were conducted using SPSS version 18.0 (SPSS Inc., Chicago, IL, USA).

Exploratory associations between MRS measures and clinical variables

With a sample size of, at most, 15 subjects per group, this study did not have sufficient statistical power to enable the assessment of within-group correlations, which we estimate would require 40 or more subjects per group to be meaningful. However, because most of the clinical variables were dimensional or continuous, rather than categorical, and none of these variables had been specified as inclusion or exclusion criteria for any of the groups, the full range of clinical scores remained possible for any of the participants after enrollment (i.e. a subject who met the eligibility criteria for the HV group could still score poorly in a given clinical test). Therefore, to increase the statistical power to test for potential associations between the continuous MRS measures and the dimensional clinical scores, the full participant sample was treated as a continuum, with no *a priori* assumptions about group membership other than recognizing that there would be a 'ceiling effect' in clinical scores because of the absence of discrete levels beyond the cut-off point representing 'normal' test results. As a result of this caveat, we only report clinical correlations that reached significance at the very conservative threshold of Pearson *r* or Spearman ρ of at least 0.5 and $p = 0.001$, except where noted. Treating the three groups as a continuum also enabled the assessment of the overlap between the outcome measures to establish their potential utility in differentiating between the groups.

RESULTS

Sample demographics and clinical characteristics

Tables 1 and 2 provide the demographic and clinical characteristics, respectively, for subjects with viable data, consisting of 15 patients with CFS, 15 with MDD and 13 HVs, after excluding five patients with MDD, one with CFS and one HV with poor quality data mainly because of severe head motion, as determined by the presence of lipid peaks in voxels outside the boundaries of the brain in the ^{1}H MRSI scans. The three groups were

comparable for age, sex, ethnicity, marital status, body mass index (BMI) and years of education (Table 1). However, they differed by race ($p = 0.001$), as the CFS group consisted of Caucasian patients only.

The CFS group showed more CFS-associated symptoms relative to both the HV ($p < 0.001$) and MDD ($p = 0.019$) groups. There was a main effect of group for depression severity ($p < 0.001$), with *post-hoc* tests showing greater QIDS-SR scores in the MDD group relative to both the CFS ($p < 0.001$) and HV ($p < 0.001$) groups. There were also more depressive symptoms in patients with CFS relative to the HV group ($p = 0.003$).

The two patient groups exhibited a high degree of functional impairment and disability relative to the HV group, as measured by the Sheehan Disability Scale, but did not differ from each other ($p = 0.233$) (Table 2). In general, health quality across multiple domains was markedly reduced in the CFS group relative to the HV and MDD groups. The CFS group reported lower physical functioning, greater physical limitations, greater fatigue, higher pain scores, lower social functioning and worse general health scores than the HV group (Table 2). The MDD group fared poorly relative to the CFS group only in emotional well-being and associated limitations, but the two groups did not differ in social functioning or overall fatigue.

Using the MFI, fatigue severity was assessed in all subjects for the following five dimensions: general fatigue (GF), physical fatigue (PF), mental fatigue (MF), reduced motivation (RM) and reduced activity (RA). There was a significant main effect of group for fatigue severity as measured along each dimension of the MFI (Table 2). *Post-hoc* testing revealed that the group differences were driven by greater fatigue in both the CFS and MDD groups relative to the HV group, without any significant difference between CFS and HV with regard to motivational level, or between CFS and MDD with regard to activity level, mental fatigue or general fatigue (Table 2).

Testing of primary hypotheses

Ventricular lactate and volume—Mean ^{1}H MRSI-derived ventricular lactate levels differed significantly (Fig. 4A) between the CFS (2.23 ± 1.10 i.u.), MDD (1.35 ± 0.93 i.u.) and HV (0.00 0.86 i.u.) groups ($F_{2,33} = 16.78$; $p < 0.001$). *Post-hoc* testing revealed significantly higher ventricular lactate levels in both CFS ($p < 0.001$) and MDD ($p = 0.009$) groups relative to HV, with a weak trend towards higher levels in CFS relative to MDD ($p = 0.114$). When controlling lactate levels for age and other covariates (gender, smoking status and BMI), the significant main effect of group remained ($F_{2,2.4} = 13.634$, p = 0.050). The means of the ventricular volumes from which the observed lactate signal was measured did not differ between the CFS (3554 ± 457 mm^3), MDD (3971 ± 643 mm^3) and HV (3057 ± 503 mm^3) groups ($p = 0.48$). As expected, there was an association between ventricular volume and age ($\rho = 0.437$, $p = 0.004$) across all participants, but ventricular lactate did not correlate with ventricular volume ($r = 0.263$, $p = 0.127$).

Occipital lobe GSH and voxel tissue heterogeneity—There was a main effect of group on occipital GSH levels normalized to the peak area of the unsuppressed voxel tissue water (W) ($F_{2,40} = 15.93$; $p < 0.001$) which, on *post-hoc* testing, was attributable to reductions in GSH/W (Fig. 4B) in both the CFS [$(1.86 \pm 0.47) \times 10^{-3}$; $p < 0.001$] and MDD [$(2.27 \pm 0.42)\ 10^{-3}$; $p = 0.004$] groups relative to HVs [$(2.92 \pm 0.59) \times 10^{-3}$]. There was a nonsignificant trend towards lower GSH/W in the CFS relative to MDD group ($p = 0.086$). Levels of the reference voxel water signal did not differ between the groups ($p > 0.5$), so that, henceforth, we use GSH to mean GSH/W. Age, gender, smoking status and BMI did not have an impact on cortical GSH differences, nor did tissue type, which did not differ

between the groups for GM (CFS, 10 021 ± 3158 mm^3; MDD, 11 280 ± 2307 mm^3; HV, 10 716 ± 2282 mm^3; $p = 0.656$) or WM (CFS, 5427 ± 1814 mm^3; MDD, 5351 ± 1889 mm^3; HV, 6197 ± 2004 mm^3; $p = 0.530$).

Additional analyses

Associations between ventricular lactate, cortical GSH and clinical variables

—We found a strong negative correlation between ventricular lac-tate and GSH across all participants ($r = –0.545$, $p = 0.001$; Fig. 5), as well as within the CFS group ($r = –0.544$, $p = 0.044$), although the latter correlation was of lower statistical significance. This inverse relationship between ventricular lactate and GSH was such that most of the clinical variables found to correlate positively or negatively with one MRS variable were inversely correlated with the other, as illustrated in Fig. 6.

Across the three groups, significant associations between GSH and the following clinical variables were found (Table 3): (i) RAND SF-36 scores showed GSH to be positively correlated with physical functioning (Spearman $\rho = 0.506$; $p = 0.001$) and physical energy ($\rho = 0.606$, $p < 0.001$); (ii) GSH was negatively correlated with general fatigue ($\rho = 0.565$, $p < 0.001$), physical fatigue ($\rho = –0.525$, $p < 0.001$) and reduced activity ($\rho = 0.508$, $p < 0.001$), as assessed by MFI; (iii) GSH was negatively correlated with physical impairment and disability ($\rho = –0.615$, $p < 0.001$), as measured by SDS; and (iv) GSH was negatively correlated with CFS symptomatology ($\rho = –0.633$, $p < 0.001$), as determined by the CDC CFS Symptom Inventory.

For ventricular lactate, likewise, multiple significant correlations, but opposite to those for GSH (Fig. 6), were found across the whole sample (Table 3). Health quality across nearly all domains of RAND SF-36 negatively correlated with ventricular lactate ($\rho = –0.601$, $p < 0.001$ for total RAND SF-36). In addition, there were significant positive correlations between ventricular lactate and general fatigue ($\rho = 0.537$, $p = 0.001$), physical fatigue ($\rho = 0.596$, $p < 0.001$) and reduced activity ($\rho = 0.496$, $p = 0.002$). Moreover, ventricular lactate positively correlated with the degree of physical impairment and disability ($\rho = 0.581$, $p < 0.001$); however, there was only a weak positive correlation between ventricular lactate and CFS symptoms ($\rho = 0.374$, $p = 0.038$).

Finally, sleep quality across all participants, as assessed by the Pittsburgh Sleep Quality Index, was negatively correlated with GSH ($r = –0.606$, $p = 0.001$) and positively correlated with ventricular lactate ($r = 0.601$, $p = 0.001$), with higher PSQI scores signifying greater sleep disturbance.

rCBF and global CBF measured by ASL MRI—Following intensity and morphological normalization and statistical analysis by Statistical Parametric Mapping software version 5, we found significantly different absolute CBF values, at a voxel-level significance threshold of $p < 0.001$, uncorrected for multiple comparisons, in two brain regions. The CFS group had lower rCBF values in the left anterior cingulate cortex ($p = 0.039$) and right lingual ($p = 0.016$) regions relative to the HV group (Fig. 7). In addition, there was a trend towards lower rCBF in the left anterior cingulate cortex in the MDD group relative to HVs ($p = 0.08$). There were no significant differences in rCBF values between the CFS and MDD groups in any brain region.

Although only two relatively limited regions emerged as having statistically significant CBF, examination of the raw values was highly suggestive of potentially more widespread hypoperfusion in patients with CFS and MDD. Figure 8 shows the percentage changes in mean rCBF (%ΔrCBF) measured relative to the HV group for and between the CFS and MDD groups (Fig. 8A), and the percentage changes in mean global CBF (%ΔgCBF)

relative to HV for and between the CFS and MDD groups (Fig. 8B). For nearly all individual regions (Fig. 8A) and globally (Fig. 8B), the mean %ΔrCBF and %ΔgCBF values for both the CFS and MDD groups were numerically lower than those for the HV group (Fig. 8A, B), whereas those for the CFS group were numerically lower than those for the MDD group. However, these numerical differences failed to reach statistical significance.

Regional brain high-energy phosphate levels measured by ^{31}P MRSI—None of the exploratory statistical analyses conducted on the levels of high-energy phosphates, including ATP, creatine phosphate (PCr) and inorganic phosphate (Pi), as well as on their ratios (e.g. ATP/PCr or Pi/Cr) and on the intracellular pH derived from Pi chemical shifts, revealed a main effect of group in any brain region. In addition, there were no correlations between any of the phosphate metabolites and demographic and clinical variables.

DISCUSSION

This report marks the third in a series of neuroimaging investigations of CFS, a disorder with an uncertain pathophysiology. In this independent cohort, we replicated our previously reported elevations of ventricular CSF lactate in patients with CFS relative to age- and sex-matched HVs. In addition, we report, for the first time, significant reductions in the levels of cortical GSH in patients with CFS and MDD relative to healthy controls. Ventricular lactate and cortical GSH were inversely correlated with each other, as well as with several key indices of physical health and disability. These findings further implicate ventricular lactate elevations in patients with CFS, whereas decreases in the antioxidant GSH in patients with CFS and MDD strongly suggest a role of increased oxidative stress in the two disorders.

Ventricular lactate elevations

Although, in the second study of this series (4), we did not find any ventricular lactate differences between HVs and patients with MDD, or between patients with CFS and MDD, despite numerically different mean values, in the present study, we found significantly higher ventricular lactate levels in patients with MDD relative to HVs, and weak trend elevations in the CFS relative to the MDD group. This may indicate that the CFS and MDD patient groups recruited for the present study were more representative of each disorder, as the CFS group exhibited more CFS symptoms (by CDC Symptom Inventory) and physical fatigue (by MFI) than did the MDD group, and patients with MDD were significantly more depressed than those with CFS (by QIDS-SR), whereas the two groups were well matched with respect to overall fatigue and functional disability (Table 2). The improved group matching might have decreased the overlap in key symptoms, thereby decreasing the heterogeneity within each group and the associated variance. These considerations suggest that higher ventricular lactate in patients with CFS than in those with MDD might be found in larger studies. However, the relatively small magnitude of the difference suggests that ventricular lactate alone is unlikely to be a biomarker for differentiating between individual patients with CFS and MDD.

Cortical GSH deficits

In this study, we found significant GSH deficits in patients with CFS and MDD relative to HVs, and a nonsignificant trend towards lower GSH in patients with CFS relative to those with MDD. To our knowledge, this is the first study to document GSH deficits in patients with MDD, consistent with recent hypotheses regarding redox dysregulation and increased oxidative stress in the disorder (29,30). Our finding of significant GSH deficits in patients with CFS is in contrast with a recent ^{1}H MRS study, which failed to detect cortical GSH differences between patients with CFS and healthy subjects (31). However, that study had a number of notable methodological limitations. First, a conventional single-voxel point-

resolved spectroscopy ^{1}H MRS technique, which does not yield a detectable GSH signal, was used to measure this weak signal in the presence of an overlapping tCr peak at 3.0 ppm (see Fig. 3B, spectrum a), which is up to 10-fold stronger, requiring spectral simulation of an invisible resonance. Second, a relatively long TE of 144 ms was used, which unavoidably led to significant losses in the signal intensity of the already weak GSH peak as a result of *J*-coupling evolution and T_2 decay. Finally, although a spectral estimation method was implemented to derive computationally the GSH peak levels despite the overlap, no spectral data showing the quality of the model fitting, or quantitative estimates of the associated errors, were provided to enable the assessment of the reliability of the fitting procedure. It is therefore highly unlikely that the reported 'GSH' values of 2.703 ± 2.311 (standard deviation) for patients with CFS and 5.191 ± 8.984 for healthy controls (31) could have been distinguished from background noise or from mixtures of overlapping and co-resonant GABA and mobile macromolecules. This is in contrast with the present study, which used a spectral editing technique that yields an unobstructed GSH peak (Fig. 3B, C), and has been employed extensively by our group (32) and others (23,33–35) to measure similarly low concentrations of brain GABA under equally challenging *in vivo* conditions.

The present ^{1}H MRS measures of brain GSH are difficult to compare with previous peripheral measures in patients with CFS, which did not differ from controls (6,36,37), as GSH has poor blood–brain barrier permeability and transport properties (38), such that blood levels may not reflect cortical levels. A consequence of the poor blood–brain barrier permeability of GSH is that dietary supplements of the antioxidant are unlikely to increase the cortical levels significantly, justifying the heightened interest in synthetic GSH precursors, such as *N*-acetylcysteine, that can cross the blood–brain barrier to spur *in situ* synthesis and elevations of cortical GSH (38). Thus, our finding of significant GSH deficits in patients with CFS relative to HVs, which correlated strongly with various indices of physical health and functional disability, suggests that the investigation of such indirect approaches for the elevation of cortical GSH for neuro-protection in CFS might be warranted.

Clinical correlations and implications of differences between CFS and MDD groups

The results of our clinical evaluations of the CFS and MDD groups were consistent with the overall manifestations of each disorder, whilst also revealing significant symptom overlap across a wide range of indices of physical and functional disability, which may account for the difficulty in differentiating between the two disorders. The two groups differed with regard to the more pronounced depressive symptoms, reduced motivation and more 'limitations due to emotional difficulties' and less 'emotional well-being' in MDD, and more pain, physical limitations and physical fatigue, and poorer general health and physical functioning, in CFS.

Although GSH correlated strongly with CFS symptoms, correlations between CFS symptoms and ventricular lactate were much weaker, potentially suggesting a tighter coupling of GSH deficits than lactate, whose elevations might be more distal to pathophysiology, with CFS symptoms. Importantly, examination of the relationships between the two MRS variables and clinical indices across the full sample (Fig. 6; Table 3) revealed such a high degree of overlap that these MRS variables, alone or in concert, cannot be considered as sensitive biomarkers of CFS or MDD, or a basis for differentiating between the two disorders. However, the fact that we found direct correlations between GSH and clinical indices of good health or function, and between ventricular lactate and indices of poor health and physical disability, across multiple domains is qualitatively consistent with the beneficial role of GSH in detoxification and in mitigating the effects of oxidative stress,

and with the role of lactate as a marker of nonsalutary biological challenge, such as defective cell energetics or infarction.

rCBF and global CBF

In this study, we found limited regions of hypoperfusion in patients with CFS relative to HVs, a finding that is in agreement with most (8–11,39), but not all (40,41), previous measurements of rCBF using single-photon emission computed tomography (SPECT) (8,9,39–41), Xe computed tomography (10) or ASL (11). In nearly all studies that found CBF deficits in patients with CFS, multiple regions were reported to be involved (8,9,11,39), with some of the regions of hypoperfusion being as small as or less than 1 cm (33). These findings of extensive areas of hypoperfusion in patients with CFS suggest that our failure to find widespread regions with decreased rCBF in this study, despite numerically lower values in patients with CFS and MDD relative to HVs (Fig. 8A, B), was probably the result of a Type II statistical error, i.e. our study was insufficiently powered to detect more widespread rCBF deficits by ASL. As in the present study, one of the published studies (41) compared rCBF in CFS, MDD and HV groups, but measured with SPECT, and found decreases in the frontal lobe in the MDD group relative to both CFS and HV groups, with no differences between the last two groups. This is qualitatively in agreement with the present study, which found a trend towards decreased anterior cingu-late cortex CBF in the MDD group, a region in which we (32) and others (33–35) have previously found significant amino acid neurotransmitter abnormalities.

It is unclear whether the degree of hypoperfusion found in patients with CFS by these multiple techniques is sufficient to trigger increased glycolytic activity that could account for our observed elevations of ventricular lactate. However, at least three threshold levels of cell hypoxia have been described (42), one of which could plausibly trigger increased glycolytic rates in patients with CFS: (i) decreased oxygen tension, but the cell's ATP production remains able to meet energy demand through changes in phosphorylation state and increased glycolysis; (ii) an oxygenation level at which steady-state ATP levels can be maintained only by increased anaerobic glycolysis through the very inefficient Embden–Meyerhof pathway, which is not sustainable in a high-energy-consuming organ, such as the brain, leading to rapid ATP depletion; and (iii) an oxygenation level at which anaerobic glycolysis is no longer able to generate sufficient ATP to maintain cell function. As we did not find deficits in ATP in this study (see Results section), and the levels of ventricular lactate measured in patients with CFS are relatively small relative to those reported previously in fully symptomatic patients with primary mitochondrial disorders (43) or cerebral infarction (44), we postulate that the observed ventricular lactate elevations may be triggered by a decrease in oxygenation level corresponding to the first aforementioned threshold level (i.e. mild to moderate hypoxia), which may result from CBF decreases found in this and previous studies (8–11,39). However, direct evidence of altered tissue oxygenation in patients with CFS is necessary to establish a definite mechanistic link between rCBF decreases and the observed lactate elevations.

Implications for the oxidative stress model of CFS

Taken in the context of recent studies reporting credible evidence of increased markers of oxidative stress in patients with CFS (6,7), the present study supports an emerging oxidative stress hypothesis (5), which implicates sustained oxidative damage as an integral aspect of CFS pathophysiology. Our findings of significant cortical GSH deficits in patients with CFS, which are associated with multiple clinical indices and physical disability, are consistent with studies showing significantly elevated levels of 8-iso-prostaglandin-$F_{2\alpha}$-isoprostanes (6,7), which are reliable blood markers of oxidative stress that are also correlated with clinical symptoms in CFS (45). Our explanatory model, depicted in Fig. 9,

shows how increased oxidative stress might relate to and/or explain our findings of elevated ventricular lactate in three independent CFS samples.

The view that oxidative stress might play a key role in the pathophysiology of CFS, first coherently advanced by Pall (5), posits that an initial infectious process or associated immuno-logic response ('cloud' in model shown in Fig. 9) induces one or more cytokines (interleukin-1, interleukin-6, tumor necrosis factor-α, interferon-γ), which, in turn, induce nitric oxide synthase, leading to increased levels of nitric oxide (·NO) that subsequently react with superoxide (·OO–) to produce peroxynitrite (OONO), a potent pro-inflammatory and pro-apoptotic reactive oxygen/nitrogen species (ROS/RNS) and mediator of oxidative stress (45,46). In the absence of adequate antioxidant defense capacity or reserves, of which GSH is the most abundant and important component, peroxynitrite (Fig. 9, left-hand pathway) will react with arachidonic acid (AA) in cell membrane phospholipids, forming isoprostanes (46,47) and compromising membrane and cell function (5,45–47). Therefore, the results of recent studies (6,7) reporting significant elevations of blood levels of isoprostanes in patients with CFS, which correlated with clinical symptoms in one study (6), represent exceptionally strong evidence for the view that oxidative stress is implicated in the disorder. Importantly, our finding of significant cortical deficits in the primary intracellular antioxidant GSH in patients with CFS has added both mechanistic and face validity to this model by establishing that oxidative stress in the disorder is, at least in part, caused by decreased antioxidant capacity.

In addition to their role as markers of oxidative stress, isoprostanes have potent vasoconstrictor effects on peripheral vasculature, including cerebral arterioles (45,46). The finding of significantly elevated levels of these byproducts of membrane lipid peroxidation in patients with CFS may therefore also explain the results of this and multiple previous studies that have found reduced absolute (10) and relative (8,9,11,39) cortical and subcortical blood flow in patients with CFS. As cerebral hypoper-fusion is known to increase brain lactate (42), our finding of elevated CSF lactate, together with previous reports of increased markers of oxidative stress and evidence of hypoperfusion in patients with CFS, suggest a pathophysiological model of the disorder (Fig. 9) in which increased oxidative stress elevates blood levels of isoprostanes, which then constrict cerebral arterioles, leading to decreased cerebral blood flow and to attendant increases in anaerobic metabolism and lactate elevations.

Finally, as oxidative stress and the associated accumulation of free radicals can lead to mitochondrial dysfunction (48), the involvement of oxidative stress in CFS also raises the possibility that the observed cross-sectional elevations of ventricular lactate could be the result of secondary mitochondrial dysfunction (Fig. 9; right-hand branch of model), which would lead to ATP and energy production deficits that would be compensated by the upregulation of glycolytic activity, with attendant lactate production. However, our measurement of ATP and other high-energy phosphates that might be affected in the case of significant mitochondrial dysfunction found no abnormalities. Therefore, the results of this study do not support a significant involvement of mitochondrial energy metabolism in CFS, although our failure to find such evidence might be caused by the reported insensitivity of the ^{31}P MRS method to subtle mitochondrial defects at rest (49,50).

Limitations

A limitation of this pilot study is that our relatively small sample size did not provide sufficient power to enable reliable assessment of within-group correlations, or to confirm more widespread regions of hypoperfusion in patients with CFS. Therefore, these results require replication in larger samples. Moreover, we did not obtain circulating levels of isoprostanes in our study participants, inferring increases in the levels of this important

component of the model from published findings, and our resting-state ^{31}P MRSI assessment of mitochondrial dysfunction is inconclusive, because of the possibility that the unmasking of subtle mitochondrial metabolism defects by this technique might require the acquisition of spectra at rest and then during and following symptom provocation or a suitable task activation (49,50). Finally, the neuroimaging outcome measures assessed in this study, individually or in combination, do not seem likely to enable individual patients with CFS and MDD to be differentiated clinically. However, the results presented here have demonstrated the high overall potential of these methods to contribute to a new pathophysiological understanding by enabling *in vivo* testing of the consistency and validity of a promising model of CFS, and by providing a compelling rationale to undertake studies to investigate neuro-protective treatments (e.g. *N*-acetylcysteine) that can elevate cortical GSH to mitigate against the effects of oxidative stress-mediated damage in the disorder.

Acknowledgments

Contract/grant sponsors included the Chronic Fatigue and Immune Dysfunction Syndrome (CFIDS) Association of America, Inc. and the National Institutes of Health (contract/grant number: R01 MH-075895, K23 MH-069656).

We thank the patients who participated in this study and their families, and Mr Josefino Borja for his valuable contribution in operating the MRI scanner.

Abbreviations used

AA	arachidonic acid
ANOVA	analysis of variance
ASL	arterial spin labeling
BMI	body mass index
CDC	US Centers for Disease Control and Prevention
CFS	chronic fatigue syndrome
CSF	cerebrospinal fluid
GABA	γ-aminobutyric acid
GM	gray matter
GSH	glutathione
HV	healthy volunteer
MDD	major depressive disorder
MFI	Multidimensional Fatigue Inventory
MFI GF	Multidimensional Fatigue Inventory general fatigue
MFI MF	Multidimensional Fatigue Inventory mental fatigue
MFI PF	Multidimensional Fatigue Inventory physical fatigue
MFI RA	Multidimensional Fatigue Inventory reduced activity
MFI RM	Multidimensional Fatigue Inventory reduced motivation
OCC	occipital cortex
QIDS-SR	Quick Inventory of Depressive Symptomatology – Self Report

RAND GH	general health survey by the RAND Corporation, Santa Monica, CA, USA
RAND SF	RAND social functioning survey
RAND SF-36	RAND 36-Item Short Form Health Survey
rCBF	regional cerebral blood flow
RF	radiofrequency
ROS/RNS	reactive oxygen/nitrogen species
SDS	Sheehan Disability Scale
SPECT	single-photon emission computed tomography
tCr	total creatine
WM	white matter

REFERENCES

1. Fukuda K, Straus SE, Hickie I, Sharpe MC, Dobbins JG, Komaroff A. The chronic fatigue syndrome: a comprehensive approach to its definition and study. International chronic fatigue syndrome study group. Ann. Intern. Med. 1994; 121:953–959. [PubMed: 7978722]
2. Afari N, Buchwald D. Chronic fatigue syndrome: a review. Am. J. Psychiatry. 2003; 160:221–236. [PubMed: 12562565]
3. Mathew SJ, Mao X, Keegan KA, Levine SM, Smith EL, Heier LA, Otcheretko V, Coplan JD, Shungu DC. Ventricular cerebrospinal fluid lactate is increased in chronic fatigue syndrome compared with generalized anxiety disorder: an *in vivo* 3.0 T ^{1}H MRS imaging study. NMR Biomed. 2009; 22:251–258. [PubMed: 18942064]
4. Murrough JW, Mao X, Collins KA, Kelly C, Andrade G, Nedstadt P, Levine SM, Mathew SJ, Shungu DC. Increased ventricular lactate in chronic fatigue syndrome measured by ^{1}H MRS imaging at 3 T. II: comparison with major depressive disorder. NMR Biomed. 2010; 23:643–650. [PubMed: 20661876]
5. Pall ML. Elevated, sustained peroxynitrite levels as the cause of chronic fatigue syndrome. Med. Hypotheses. 2000; 54:115–125. [PubMed: 10790736]
6. Kennedy G, Spence VA, McLaren M, Hill A, Underwood C, Belch JJ. Oxidative stress levels are raised in chronic fatigue syndrome and are associated with clinical symptoms. Free Radic. Biol. Med. 2005; 39:584–589. [PubMed: 16085177]
7. Robinson M, Gray SR, Watson MS, Kennedy G, Hill A, Belch JJ, Nimmo MA. Plasma IL-6, its soluble receptors and F-isoprostanes at rest and during exercise in chronic fatigue syndrome. Scand. J. Med. Sci. Sports. 2009; 13:1–9.
8. Ichise M, Salit IE, Abbey SE, Chung DG, Gray B, Kirsh JC, Freedman M. Assessment of regional cerebral perfusion by 99Tcm-HMPAO SPECT in chronic fatigue syndrome. Nucl. Med. Commun. 1992; 13:767–772. [PubMed: 1491843]
9. Schwartz RB, Garada BM, Komaroff AL, Tice HM, Gleit M, Jolesz FA, Holman BL. Detection of intracranial abnormalities in patients with chronic fatigue syndrome: comparison of MR imaging and SPECT. Am. J. Roentgenol. 1994; 162:935–941. [PubMed: 8141020]
10. Yoshiuchi K, Farkas J, Natelson BH. Patients with chronic fatigue syndrome have reduced absolute cortical blood flow. Clin. Physiol. Funct. Imaging. 2006; 26:83–86. [PubMed: 16494597]
11. Biswal B, Kunwar P, Natelson BH. Cerebral blood flow in chronic fatigue syndrome assessed by arterial spin labeling. J. Neurol. Sci. 2010; 301:9–11. [PubMed: 21167506]
12. Bains JS, Shaw CA. Neurodegenerative disorders in humans: the role of glutathione in oxidative stress-mediated neuronal death. Brain Res. Brain Res. Rev. 1997; 25:335–358. [PubMed: 9495562]

13. Detre JA, Alsop DC. Perfusion magnetic resonance imaging with continuous arterial spin labeling: methods and clinical applications in the central nervous system. Eur. J. Radiol. 1999; 30:115–124. [PubMed: 10401592]

14. First, MB.; Spitzer, RL.; Gibbon, M.; Williams, JBW. Structured Clinical Interview for DSM-IV Axis Disorders (SCID). New York State Psychiatric Institute, Biometrics Research; New York: 1995.

15. Smets EM, Garssen B, Bonke B, De Haes JC. The multidimensional fatigue inventory (MFI) psychometric qualities of an instrument to assess fatigue. J. Psychosom. Res. 1995; 39:315–325. [PubMed: 7636775]

16. Hays RD, Sherbourne CD, Mazel RM. The RAND 36-Item Health Survey 1.0. Health Econ. 1993; 2:217–227. [PubMed: 8275167]

17. Sheehan DV, Harnett-Sheehan K, Raj BA. The measurement of disability. Int. Clin. Psychopharmacol. 1996; 11(Suppl. 3):89–95. [PubMed: 8923116]

18. Cleeland CS, Ryan KM. Pain assessment: global use of the Brief Pain Inventory. Ann. Acad. Med. Singapore. 1994; 23(2):129–138. [PubMed: 8080219]

19. Buysse DJ, Reynolds CF 3rd, Monk TH, Berman SR, Kupfer DJ. The Pittsburgh Sleep Quality Index: a new instrument for psychiatric practice and research. Psychiatry Res. 1989; 28(2):193–213. [PubMed: 2748771]

20. Rush AJ, Trivedi MH, Ibrahim HM, Carmody TJ, Arnow B, Klein DN, Markowitz JC, Ninan PT, Kornstein S, Manber R, Thase ME, Kocsis JH, Keller MB. The 16-Item Quick Inventory of Depressive Symptomatology (QIDS), clinician rating (QIDS-C), and self-report (QIDS-SR): a psychometric evaluation in patients with chronic major depression. Biol. Psychiatry. 2003; 54:573–583. Erratum in Biol. Psychiatry, 2003; 54: 585. [PubMed: 12946886]

21. Bernstein DP, Fink L, Handelsman L, Foote J, Lovejoy M, Wenzel K, Sapareto E, Ruggiero J. Initial reliability and validity of a new retrospective measure of child abuse and neglect. Am. J. Psychiatry. 1994; 151:1132–1136. [PubMed: 8037246]

22. Duyn JH, Gillen J, Sobering G, van Zijl PC, Moonen CT. Multisection proton MR spectroscopic imaging of the brain. Radiology. 1993; 188:277–282. [PubMed: 8511313]

23. Rothman DL, Petroff OAC, Behar KL, Mattson RH. Localized ^{1}H NMR measurements of γ-aminobutyric acid in human brain in vivo. Proc. Natl. Acad. Sci. USA. 1993; 90:5662–5666. [PubMed: 8516315]

24. Terpstra M, Henry PG, Gruetter R. Measurement of reduced glutathione (GSH) in human brain using LCModel analysis of difference-edited spectra. Magn. Reson. Med. 2003; 50:19–23. [PubMed: 12815674]

25. Markwardt, CB. Non-linear least squares fitting in IDL with MPFIT.. In: Bohlender, D.; Dowler, P.; Durand, D., editors. Proceedings of Astronomical Data Analysis Software and Systems XVIII. Vol. 411. Astronomical Society of the Pacific; Quebec City, QC, Canada: San Francisco: 2009. p. 251-254.2008, *ASP Conference Series* The IDL fitting routine, 'MPFIT', is available at http://purl.com/net/mpfit, Last Modified on 21 December 2011 by Craig Markwardt

26. Marshall I, Bruce SD, Higinbotham J, MacLullich A, Wardlaw JM, Ferguson KJ, Seckl J. Choice of spectroscopic lineshape model affects metabolite peak areas and area ratios. Magn. Reson. Med. 2000; 44:646–649. [PubMed: 11025522]

27. Doyle TJ, Bedell BJ, Narayana PA. Relative concentrations of proton MR visible neurochemicals in gray and white matter in human brain. Magn. Reson. Med. 1995; 33:755–759. [PubMed: 7651110]

28. Hetherington HP, Pan JW, Mason GF, Adams D, Vaughn MJ, Twieg DB, Pohost GM. Quantitative ^{1}H spectroscopic imaging of human brain at 4.1 T using image segmentation. Magn. Reson. Med. 1996; 36:21–29. [PubMed: 8795016]

29. Ng F, Berk M, Dean O, Bush AI. Oxidative stress in psychiatric disorders: evidence base and therapeutic implications. Int. J. Neuropsychopharm. 2008; 11:851–876.

30. Michel TM, Frangou S, Thiemeyer D, Camara S, Jecel J, Nara K, Brunklaus A, Zoechling R, Riederer P. Evidence for oxidative stress in the frontal cortex in patients with recurrent depressive disorder – a postmortem study. Psychiatry Res. 2007; 151:145–150. [PubMed: 17296234]

31. Puri BK, Agour M, Gunatilale KDR, Fernando KAC, Gurusinghe AI, Treasaden IH. An in vivo proton neurospectroscopy study of cerebral oxidative stress in myalgic encephalomyelitis (chronic fatigue syndrome). Prostaglandins Leukot. Essent. Fatty Acids. 2009; 81:303–305. [PubMed: 19906518]
32. Price RB, Shungu DC, Mao X, Nestadt P, Kelly C, Collins KA, Murrough JW, Charney DS, Mathew SJ. Amino acid neurotransmitters assessed by proton magnetic resonance spectroscopy: relationship to treatment resistance in major depressive disorder. Biol. Psychiatry. 2009; 65:792–800. [PubMed: 19058788]
33. Sanacora G, Gueorguieva R, Epperson CN, Wu YT, Appel M, Rothman DL, Krystal JH, Mason GF. Subtype-specific alterations of gamma-aminobutyric acid and glutamate in patients with major depression. Arch. Gen. Psychiatry. 2004; 61:705–713. [PubMed: 15237082]
34. Bhagwagar Z, Wylezinska M, Jezzard P, Evans J, Boorman EM, Matthews PJ, Cowen P. Low GABA concentrations in occipital cortex and anterior cingulate cortex in medication-free, recovered depressed patients. Int. J. Neuropsychopharmacol. 2008; 11:255–260. [PubMed: 17625025]
35. Hasler G, van der Veen JW, Tumonis T, Meyers N, Shen J, Drevets WC. Reduced prefrontal glutamate/glutamine and gamma-aminobutyric acid levels in major depression determined using proton magnetic resonance spectroscopy. Arch. Gen. Psychiatry. 2007; 64:193–200. [PubMed: 17283286]
36. Richards RS, Roberts TK, McGregor NR, Dunstan RH, Butt HL. Blood parameters indicative of oxidative stress are associated with symptom expression in chronic fatigue syndrome. Redox Rep. 2000; 5:35–41. [PubMed: 10905542]
37. Manuel Y, Keenoy B, Moorkens G, Vertommen J, Noe M, Ne've J, De Leeuw I. Magnesium status and parameters of oxidant–antioxidant balance in patients with chronic fatigue syndrome. J. Am. Coll. Nutr. 2000; 19:374–382. [PubMed: 10872900]
38. Zeevalk GD, Razmpour R, Bernard LP. Glutathione and Parkinson's disease: is this the elephant in the room? Biomed. Pharmacother. 2008; 62:236–249. [PubMed: 18400456]
39. Costa DC, Tannock C, Brostoff J. Brainstem perfusion is impaired in chronic fatigue syndrome. Q. J. Med. 1997; 88:767–773.
40. Lewis DH, Mayberg HS, Fischer ME, Goldberg J, Ashton S, Graham MM, Buchwald D. Monozygotic twins discordant for chronic fatigue syndrome: regional cerebral blood flow SPECT. Radiology. 2001; 219:766–773. [PubMed: 11376266]
41. Fischler B, D'Haenen H, Cluydts R, Michiels V, Demets K, Bossuyt A, Kaufman L, De Meirleir K. Comparison of 99 m Tc HMPAO SPECT scan between chronic fatigue syndrome, major depression and healthy controls: an exploratory study of clinical correlates of regional cerebral blood flow. Neuropsychobiology. 1996; 34:175–183. [PubMed: 9121617]
42. Connett RJ, Honig CR, Gayeski TE, Brooks GA. Defining hypoxia: a systems view of VO_2, glycolysis, energetics, and intracellular PO_2. J. Appl. Physiol. 1990; 68:833–842. [PubMed: 2187852]
43. Kaufmann P, Shungu DC, Sano MC, Jhung S, Engelstad K, Mitsis E, Mao X, Shanske S, Hirano M, DiMauro S, De Vivo DC. Cerebral lactic acidosis correlates with neurological impairment in MELAS. Neurology. 2004; 62:1297–1302. [PubMed: 15111665]
44. Federico F, Conte C, Simone IL, Giannini P, Liguori M, Picciola E, Tortorella C, Ferrari E. Proton magnetic resonance spectroscopy in patients with ischemic stroke. Ital. J. Neurol. Sci. 1994; 15:413–420. [PubMed: 7875959]
45. Basu S. F_2-Isoprostanes in human health and diseases: from molecular mechanisms to clinical implications. Antioxid. Redox Signaling. 2008; 10:1405–1434.
46. Salvemini D, Doyle TM, Cuzzocrea S. Superoxide, peroxynitrite and oxidative/nitrative stress in inflammation. Biochem. Soc. Trans. 2006; 34:965–970. [PubMed: 17052238]
47. Hoffman SW, Moore S, Ellis EF. Isoprostanes. Free radical-generated prostaglandins with constrictor effects on cerebral arterioles. Stroke. 1997; 28:844–849. [PubMed: 9099206]
48. Zeevalk GD, Bernard LP, Song C, Gluck M, Ehrhart J. Mitochondrial inhibition and oxidative stress: reciprocating players in neurodegeneration. Antioxid. Redox Signal. 2005; 7:1117–1139. [PubMed: 16115016]

49. Rango M, Bozzali M, Prelle A, Scarlato G, Bresolin N. Brain activation in normal subjects and in patients affected by mitochondrial disease without clinical central nervous system involvement: a phosphorus magnetic resonance spectroscopy study. J. Cerebr. Blood Flow Metab. 2001; 21:85–91.

50. Rango M, Bonifati C, Bresolin N. Parkinson's disease and brain mitochondrial dysfunction. A functional phosphorus magnetic resonance spectroscopy study. J. Cerebr. Blood Flow Metab. 2006; 26:283–290.

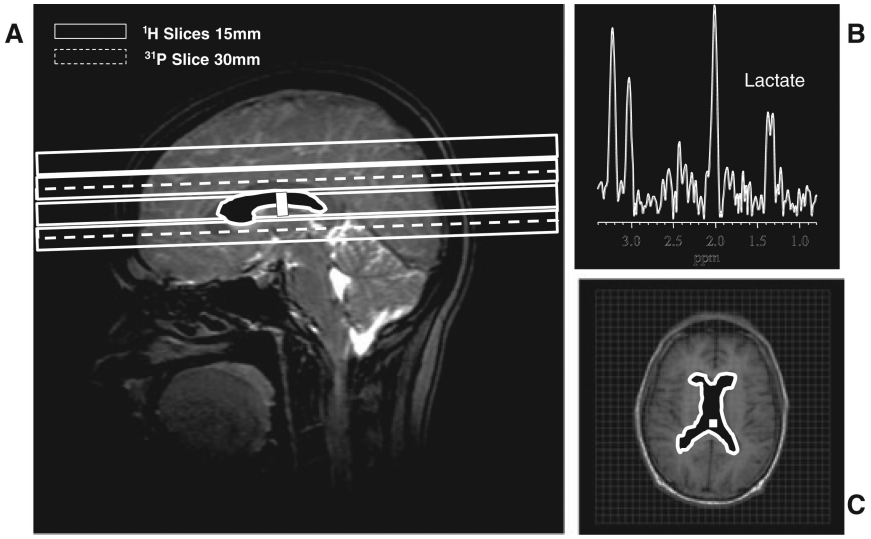

Figure 1.

(A) Prescription of the slice(s) of interest for ^{1}H and ^{31}P MRSI scans. (B) Sample ^{1}H spectrum from a voxel (see box in A) in the lateral ventricle of a patient with chronic fatigue syndrome (CFS) showing a clear lactate doublet peak at 1.33 ppm; also shown are contaminating resonances for *N*-acetylaspartate (NAA), total creatine (tCr) and total choline (tCho) from surrounding brain tissue as a result of partial volume averaging. (C) The filled structure, which is also shown in (A), depicts the ventricular region of interest from which lactate levels were obtained. The volume of this region of interest was determined by manual delineation of tissue-segmented volumetric MR images to enable the adjustment of lactate for partial volume effects.

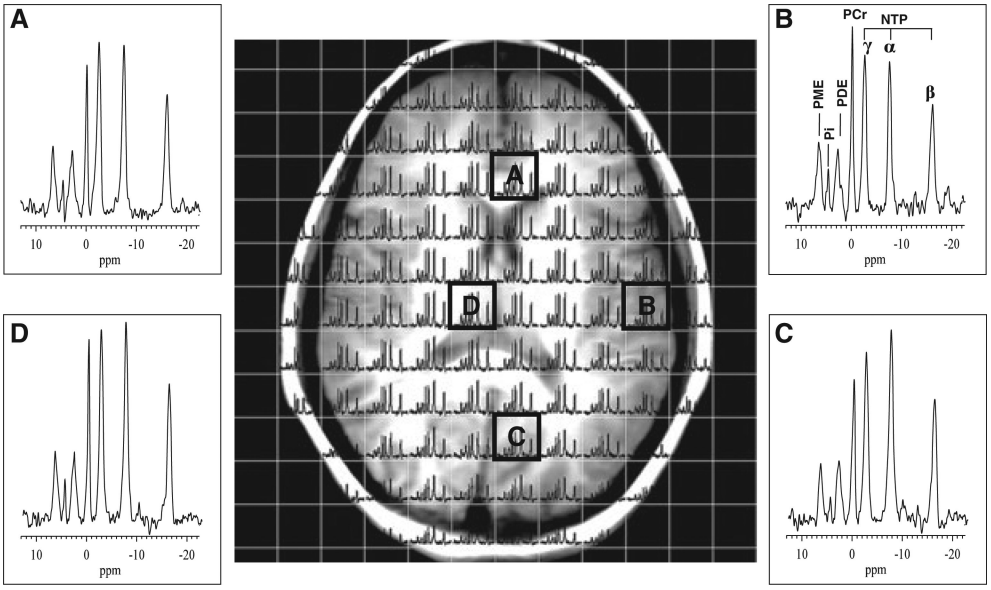

Figure 2.

Sample ^{31}P MRSI grid overlaid on a corresponding axial-oblique localizer MR image. Insets show the spectral quality for several voxels across the brain. Baseline distortions in each spectrum introduced by the large first-order phase corrections needed to account for the finite delay between the single slice-selective excitation pulse and signal acquisition were removed by interpolation. The following phosphate resonances are identified (inset B): phosphomonoesters (PME), inorganic orthophosphate (Pi), phosphodiesters (PDE), phosphocreatine (PCr) and the α, β and γ moieties of nucleoside triphosphate (NTP).

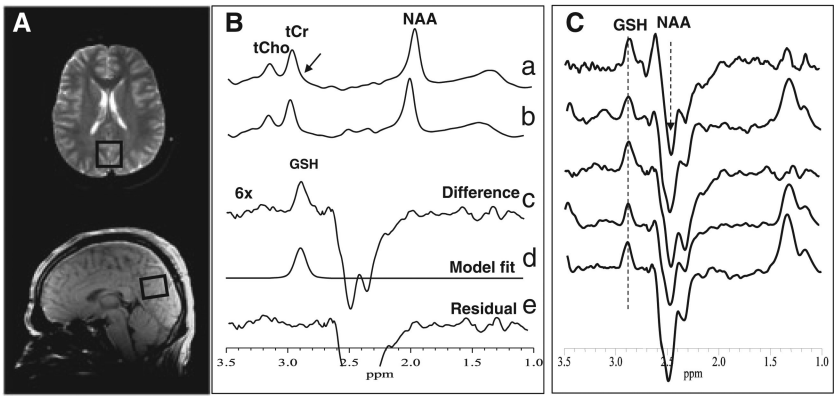

Figure 3.

(A) Location of a 2.0 × 3.0 × 3.0-cm^3 occipital lobe voxel in which glutathione (GSH) was measured. (B) Demonstration of *in vivo* human brain GSH detection by ^{1}H MRS: spectra a and b, single-voxel subspectra acquired in 15 min with the editing pulse on and off and 290 (580 total) interleaved averages; spectrum c, difference between spectra a and b showing the edited brain GSH resonance; spectrum d, model fitting of spectrum c to obtain the GSH peak area; spectrum e, residual of the difference between spectra c and d. (C) Stacked plots of edited spectra obtained as in (B) from five randomly selected subjects showing clear and consistent detection of GSH. NAA, *N*-acetylaspartate; tCho, total choline; tCr, total creatine.

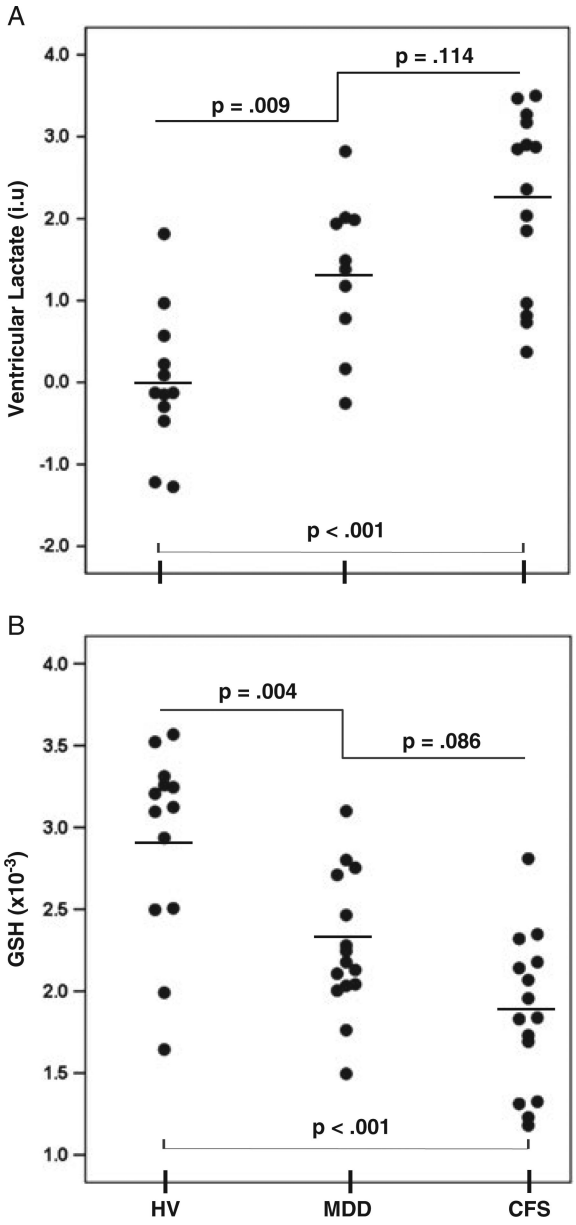

Figure 4.

Scatter plots comparing ventricular lactate (A) and occipital glutathione (GSH) levels (B) in patients with chronic fatigue syndrome (CFS) or major depressive disorder (MDD) and in healthy volunteers (HV).

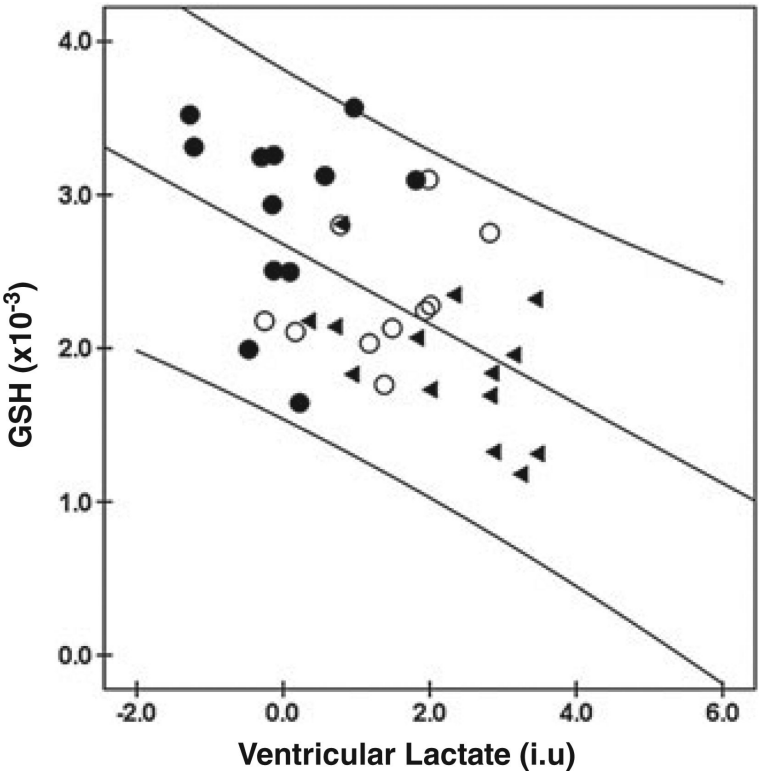

Figure 5.
Correlation of occipital glutathione (GSH) and ventricular lac-tate levels across all chronic fatigue syndrome (CFS) (▶), major depressive disorder (MDD) (○) and healthy volunteer (HV) (●) groups.

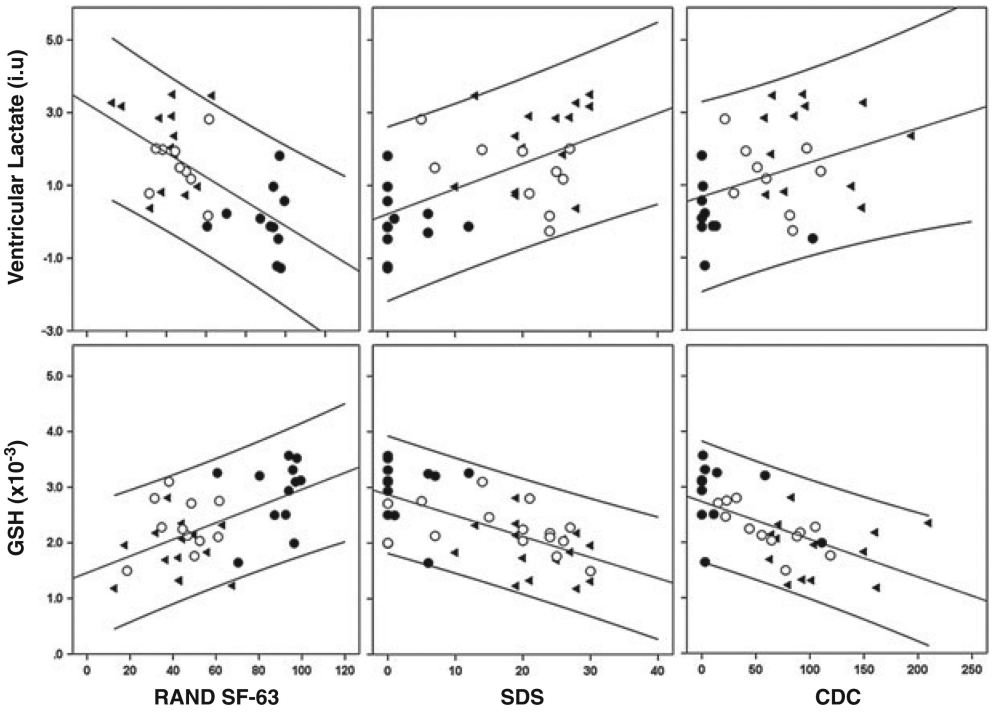

Figure 6.

Associations between ventricular lactate and glutathione (GSH) in chronic fatigue syndrome (CFS) (▶), major depressive disorder (MDD) (○) and healthy volunteer (HV) (●) groups and the following selected clinical variables: (A) total RAND SF-36 (36-Item Short Form Health Survey by the RAND Corporation, Santa Monica, CA, USA) scores; (B) Sheehan Disability Scale (SDS); (C) US Centers for Disease Control and Prevention (CDC) CFS Symptom Inventory.

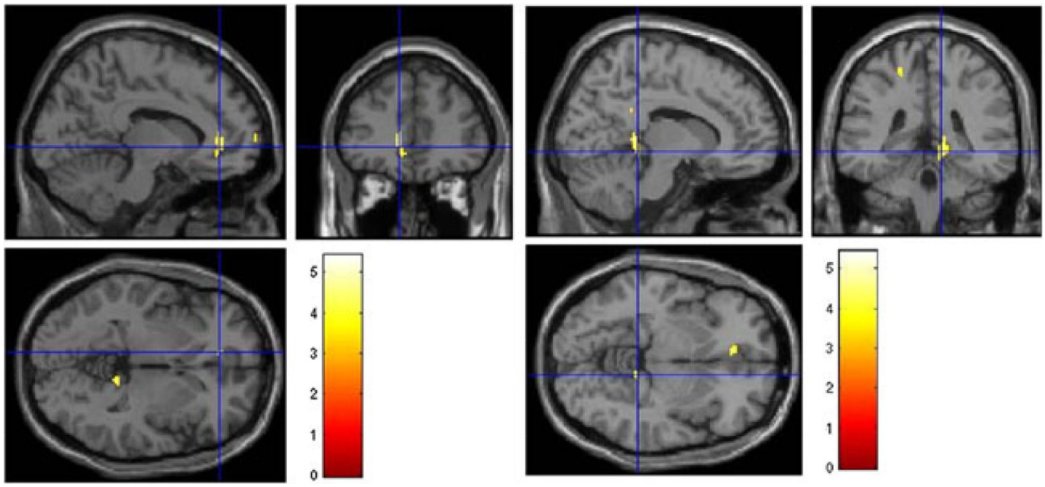

Figure 7.
Regional cerebral blood flow (rCBF) maps showing regions of statistically significant hypoperfusion in patients with chronic fatigue syndrome (CFS) relative to healthy volunteers (HV): left panel, left anterior cingulate cortex ($p = 0.039$); right panel, right lingual region ($p = 0.016$).

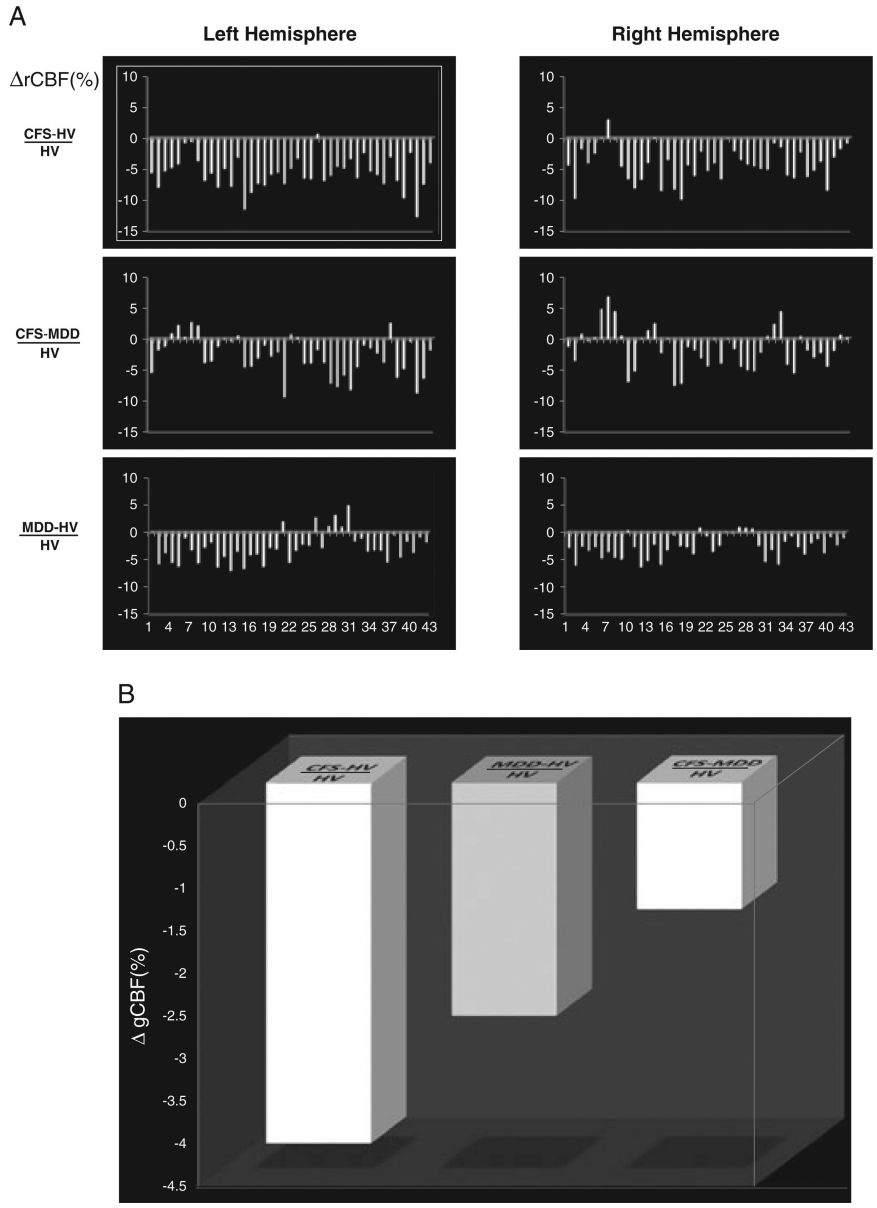

Figure 8.

(A) Percentage regional cerebral blood flow (rCBF) changes (%ΔrCBF) between CFS and HV, CFS and MDD, and MDD and HV, normalized to HV, in 43 brain regions across both hemispheres. For nearly all regions, rCBF changes vary numerically as CFS < MDD < HV. (B) Comparison of mean percentage global CBF change (%ΔgCBF) between CFS and HV, MDD and HV, and CFS and MDD. CFS, chronic fatigue syndrome; HV, healthy volunteer; MDD, major depressive disorder.

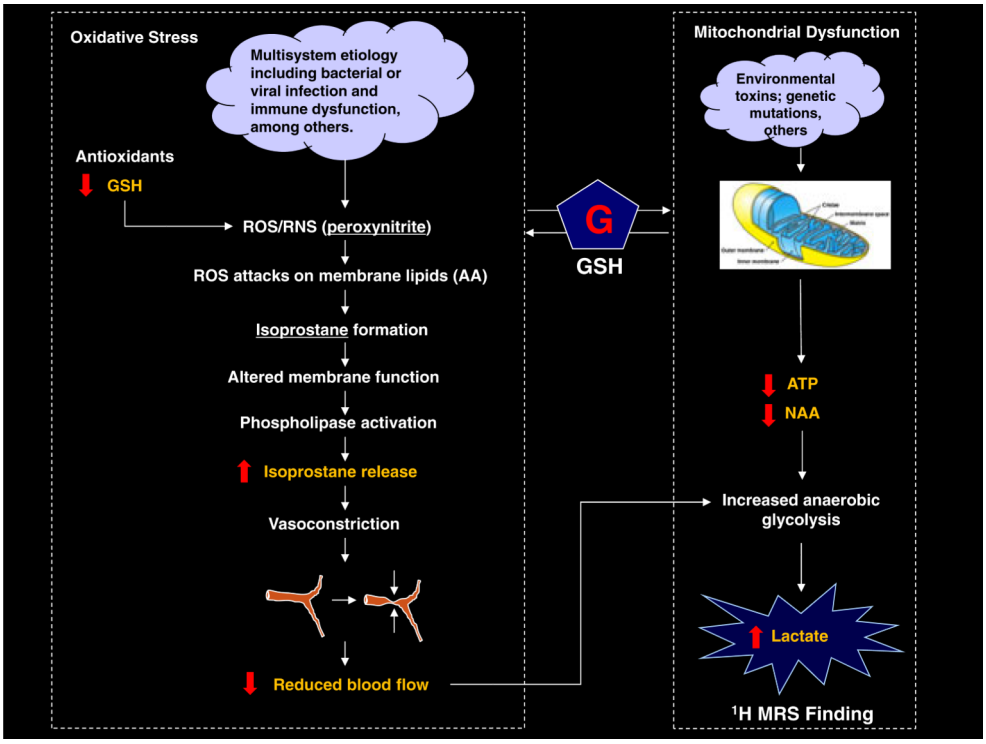

Figure 9.

Proposed pathophysiological model of chronic fatigue syndrome (CFS) investigated in this study, which may explain the observed cross-sectional elevations of ventricular lactate. Highlighted are the experimentally measurable items, with the red arrows showing the model-predicted outcomes. In this and in two previous studies (3,4), we aimed to validate the model by measuring each item and comparing the results with the predictions, except for the isoprostanes, which have been reported previously (6,7) to be increased significantly in CFS (see text for details). AA, arachidonic acid; GSH, glutathione; NAA, *N*-acetylaspartate; ROS/RNS, reactive oxygen/nitrogen species;

Table 1

Demographic characteristics

Characteristic	HV	MDD	CFS	Test statistic, *p* value
Age (years)[a] (SD)	27.6 (7.4)	31.7 (9.6)	32.7 (8.6)	H(2) = 2.114, $p = 0.347$
Female (%)	7/13 (53.8)	9/15 (60)	12/15 (80)	$\chi^2(2, n = 43) = 2.36$, $p = 0.307$
Race (%)				$\chi^2(6, n = 41) = 21.55$, $p = 0.001$
Caucasian	7/13 (53.8)	6/15 (40)	15/15 (100)	
Asian	3/13 (23.1)	0/15	0/15	
Black	1/13 (7.7)	6/15 (40)	0/15	
Other	1/13 (7.7)	2/15 (13.3)	0/15	
Missing	1/13 (7.7)	1/15 (6.7)	0/15	
Ethnicity (%)				$\chi^2(2, n = 41) = 2.46$, $p = 0.293$
Hispanic	2/13 (15.4)	4/15 (26.7)	1/15 (6.7)	
Non-Hispanic	10/13 (76.9)	9/15 (60)	14/15 (93.3)	
Missing	1/13 (7.7)	1/15 (6.7)	0/15	
Current status (%)				$\chi^2(2, n = 41) = 2.10$, $p = 0.349$
Smoker	1/13 (7.7)	4/15 (26.7)		
Nonsmoker	11/13 (84.6)	10/15 (66.7)	2/15 (13.3)	
Missing	1/13 (7.7)	1/15 (6.7)	13/15 (86.7)	
Marital status (%)	1/13 (7.7)	1/15 (6.7)	1/15 (6.7)	$\chi^2(2, n = 43) = 1.14$, $p = 0.565$
Married				
Body mass index (SD)	23.0 (2.9)	24.0 (4.0)	22.8 (3.2)	H(2) = 0.715, $p = 0.700$
Duration of illness (years) (SD)	n/a	8.8 (5.5)	9.7 (9.1)	H(1) = 0.016, $p = 0.899$
Years of education (SD)	15.6 (3.4)	17.1 (3.7)	16.0 (5.2)	H(2) = 1.014, $p = 0.602$

CFS, chronic fatigue syndrome; HV, healthy volunteer; MDD, major depressive disorder; SD, standard deviation.

[a]Inclusion age range was 18–45 years, however, one patient with MDD was aged 52 years, one with CFS was 51 years and one HV was 46 years.

Table 2

Clinical characteristics

Characteristic	HV	MDD	CFS	Global test	*Post-hoc*	*Post-hoc*	*Post-hoc*
					HV *versus* MDD	HV *versus* CFS	MDD *versus* CFS
CDC (SD)	18.3 (35.2)	61.4 (35.0)	108.6 (46.8)	H(2) = 17.882, $p < 0.001$	$U = 17.0$, $p = 0.002$	$U = 9.0$, $p < 0.001$	$U = 35.5$, $p = 0.019$
SDS (SD)	2.5 (4.0)	17.2 (9.9)	22.3 (6.1)	H(2) = 22.051, $p < 0.001$	$U = 23.5$, $p < 0.001$	$U = 1.0$, $p < 0.001$	$U = 83.0$, $p = 0.233$
QIDS (SD)	3.2 (3.8)	16.5 (4.3)	7.8 (4.3)	H(2) = 27.852, $p < 0.001$	$U = 3.0$, $p < 0.001$	$U = 35.0$, $p < 0.001$	$U = 17.0$, $p < 0.001$
WBPI (SD)	1.9 (3.9)	4.1 (10.4)	16.4 (9.3)	H(2) = 15.193, $p = 0.001$	$U = 71.0$, $p = 0.728$	$U = 19.0$, $p < 0.001$	$U = 28.0$, $p = 0.005$
PSQI (SD)	4.0 (3.3)	10.8 (2.6)	13.3 (4.5)	$F(2,34) = 22.294$, $p < 0.001$	Tukey's HSD, $p < 0.001$	Tukey's HSD, $p < 0.001$	Tukey's HSD, $p = 0.182$
Total CTQ (SD)	262 (13)	283.3 (56.9)	246.9 (61.1)	H(2) = 0.756, $p = 0.685$	n/a	n/a	n/a
RAND PF (SD)	96.2 (5.8)	77.9 (19.8)	49.0 (25.5)	H(2) = 23.776, $p < 0.001$	$U = 31.0$, $p = 0.003$	$U = 4.5$, $p < 0.001$	$U = 37.5$, $p = 0.002$
RAND phys. limit. (SD)	92.3 (12.0)	55.3 (40.6)	18.3 (35.9)	H(2) = 18.061, $p < 0.001$	$U = 40.0$, $p = 0.012$	$U = 17.0$, $p < 0.001$	$U = 55.5$, $p = 0.029$
RAND emot. limit. (SD)	87.2 (25.6)	4.8 (12.1)	77.8 (34.9)	H(2) = 26.502, $p < 0.001$	$U = 2.0$, $p < 0.001$	$U = 82.0$, $p = 0.496$	$U = 16.0$, $p < 0.001$
RAND fatigue (SD)	70.0 (26.4)	23.2 (15.6)	19.3 (18.0)	H(2) = 18.280, $p < 0.001$	$U = 11.0$, $p < 0.001$	$U = 15.0$, $p < 0.001$	$U = 90.5$, $p = 0.533$
RAND emot. well-being (SD)	88.3 (16.0)	26.7 (15.3)	68.5 (24.3)	H(2) = 26.290, $p < 0.001$	$U = 2.0$, $p < 0.001$	$U = 36.0$, $p = 0.007$	$U = 15.5$, $p < 0.001$
RAND SF (SD)	94.8 (8.4)	39.3 (24.9)	33.0 (21.1)	H(2) = 24.599, $p < 0.001$	$U = 2.5$, $p < 0.001$	$U = 0.0$, $p < 0.001$	$U = 85.5$, $p = 0.571$
RAND pain (SD)	89.8 (12.3)	76.6 (18.5)	42.2 (23.3)	H(2) = 21.578, $p < 0.001$	$U = 47.5$, $p = 0.060$	$U = 6.0$, $p < 0.001$	$U = 29.0$, $p = 0.001$
RAND GH (SD)	85.8 (18.3)	51.6 (20.5)	28.2 (19.8)	H(2) = 21.699, $p < 0.001$	$U = 22.0$, $p = 0.001$	$U = 4.0$, $p < 0.001$	$U = 45.0$, $p = 0.014$
RAND total (SD)				H(2) = 22.616, $p < 0.001$	$U = 2.0$, $p < 0.001$	$U = 2.0$, $p < 0.001$	$U = 66.0$, $p = 0.572$
MFI RA (SD)	7.9 (2.9)	14.5 (4.2)	15.4 (4.3)	H(2) = 16.895, $p < 0.001$	$U = 19.5$, $p < 0.001$	$U = 17.5$, $p < 0.001$	$U = 83.0$, $p = 0.525$
MFI MF (SD)	8.4 (5.2)	14.8 (6.6)	14.5 (4.6)	H(2) = 8.749, $p = 0.013$	$U = 43.0$, $p = 0.034$	$U = 34.5$, $p = 0.003$	$U = 83.5$, $p = 0.525$
MFI PF (SD)	6.8 (2.7)	12.4 (4.4)	16.3 (3.4)	H(2) = 21.887, $p < 0.001$	$U = 24.5$, $p = 0.001$	$U = 6.0$, $p < 0.001$	$U = 47.0$, $p = 0.019$
MFI RM (SD)	6.6 (3.5)	14.3 (3.6)	9.1 (3.5)	H(2) = 18.159, $p < 0.001$	$U = 12.0$, $p < 0.001$	$U = 56.5$, $p = 0.058$	$U = 28.5$, $p = 0.001$
MFI GF (SD)	8.2 (4.5)	16.0 (3.0)	17.0 (2.8)	H(2) = 19.804, $p < 0.001$	$U = 15.5$, $p < 0.001$	$U = 11.5$, $p < 0.001$	U = 75.5, p = .316

CDC, US Centers for Disease Control and Prevention; CFS, chronic fatigue syndrome; CTQ, Childhood Trauma Questionnaire; HSD, honestly significant difference; HV, healthy volunteer; MDD, major depressive disorder; MFI, Multidimensional Fatigue Inventory; MFI GF, Multidimensional Fatigue Inventory general fatigue; MFI MF, Multidimensional Fatigue Inventory mental fatigue; MFI PF, Multidimensional Fatigue Inventory physical fatigue; MFI RA, Multidimensional Fatigue Inventory reduced activity; MFI RM, Multidimensional Fatigue Inventory reduced motivation; PSQI, Pittsburgh Sleep Quality Index; QIDS, Quick Inventory of Depressive Symptomatology; RAND GH, general health survey by the RAND Corporation, Santa Monica, CA, USA; RAND PF, RAND physical functioning survey; RAND SF, RAND social functioning survey; SDS, Sheehan Disability Scale; WBPI, Wisconsin Brief Pain Inventory.

Table 3

Correlations between MRS and clinical variables

	Glutathione (GSH)/water in occipital region of interest	Ventricular lactate
RAND survey		
Physical functioning	$\rho = 0.506$, $p = 0.001$ *	$\rho = -0.614$, $p < 0.001$ **
Limitations due to physical problems	$\rho = 0.257$, $p = 0.100$	$\rho = -0.517$, $p = 0.001$ **
Limitations due to emotional problems	$\rho = 0.196$, $p = 0.212$	$\rho = -0.229$, $p = 0.186$
Energy/fatigue	$\rho = 0.606$, $p < 0.001$ **	$\rho = -0.504$, $p = 0.002$ **
Emotional well-being	$\rho = 0.380$, $p = 0.014$ *	$\rho = -0.355$, $p = 0.039$
Social functioning	$\rho = 0.479$, $p = 0.002$ **	$\rho = -0.635$, $p < 0.001$ **
Pain	$\rho = 0.481$, $p = 0.001$ **	$\rho = -0.550$, $p = 0.001$ **
General health	$\rho = 0.419$, $p = 0.007$ **	$\rho = -0.553$, $p = 0.001$ **
Total	$\rho = 0.485$, $p = 0.002$ **	$\rho = -0.601$, $p < 0.001$ **
Multidimensional Fatigue Inventory		
Reduced activity	$\rho = -0.508$, $p = 0.001$ **	$\rho = 0.496$, $p = 0.002$ **
Mental fatigue	$\rho = -0.309$, $p = 0.049$ *	$\rho = 0.407$, $p = 0.014$ *
Physical fatigue	$\rho = -0.525$, $p < 0.001$ **	$\rho = 0.596$, $p < 0.001$ **
Reduced motivation	$\rho = -0.251$, $p = 0.114$	$\rho = 0.126$, $p = 0.466$
General fatigue	$\rho = -0.565$, $p < 0.001$ **	$\rho = 0.537$, $p = 0.001$ **
CDC	$\rho = -0.633$, $p < 0.001$ **	$\rho = 0.374$, $p = 0.038$ *
Wisconsin Brief Pain Inventory	$\rho = -0.334$, $p = 0.040$ *	$\rho = 0.275$, $p = 0.134$
Pittsburgh Sleep Quality Index	$\rho = -0.601$, $p < 0.001$ **	$\rho = 0.628$, $p < 0.001$ **
QIDS	$\rho = -0.321$, $p = 0.036$ *	$\rho = 0.323$, $p = 0.055$
Sheehan Disability Scale	$\rho = -0.615$, $p < 0.001$ **	$\rho = 0.581$, $p < 0.001$ **
Childhood Trauma Questionnaire	$\rho = 0.094$, $p = 0.603$	$\rho = -0.249$, $p = 0.193$

CDC, US Centers for Disease Control and Prevention; QIDS, Quick Inventory of Depressive Symptomatology; RAND, RAND Corporation, Santa Monica, CA, USA

* $p < 0.05$ (two-tailed).

** $p < 0.01$ (two-tailed).